Asymptotic analysis of kinematically excited dynamical systems near resonances

Roman Starosta, Grażyna Sypniewska-Kamińska & Jan Awrejcewicz

Nonlinear Dynamics
An International Journal of Nonlinear Dynamics and Chaos in Engineering Systems

ISSN 0924-090X

Nonlinear Dyn
DOI 10.1007/s11071-011-0229-6

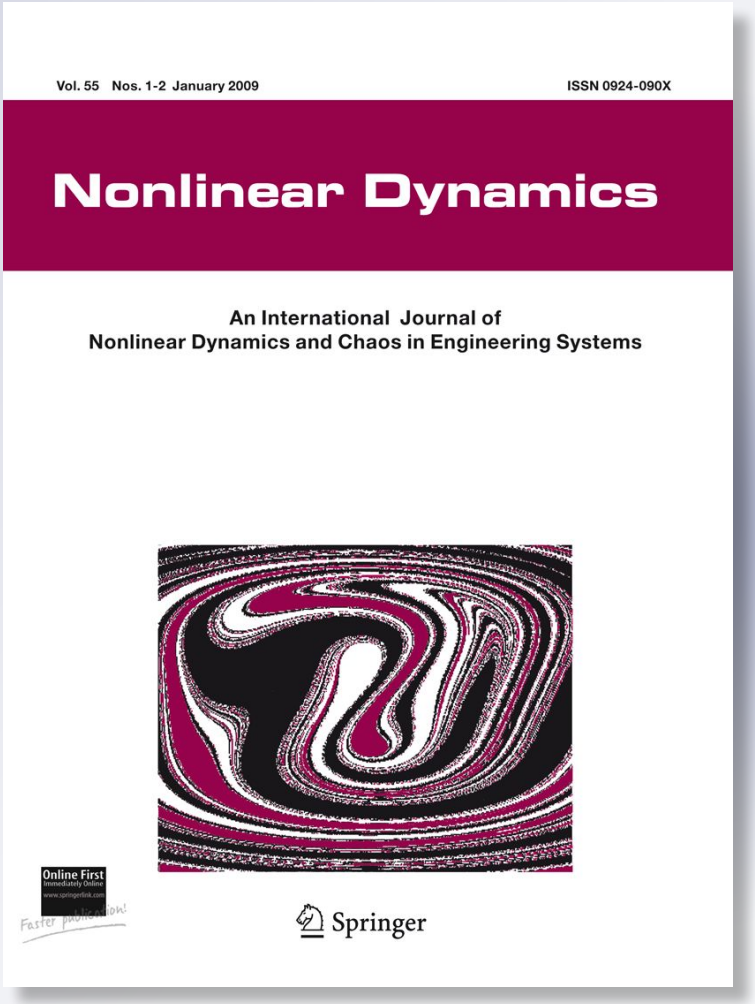

Springer

Nonlinear Dyn
DOI 10.1007/s11071-011-0229-6

ORINAL PAPER

Asymptotic analysis of kinematically excited dynamical systems near resonances

Roman Starosta · Grażyna Sypniewska-Kamińska · Jan Awrejcewicz

Received: 28 May 2011 / Accepted: 22 September 2011

Abstract The dynamic response of a harmonically and kinematically excited spring pendulum is studied. This system is a multi-degree-of-freedom system and is considered as a good example for several engineering applications. The multiple-scale (MS) method allows us to analytically solve the equations of motion and recognize resonances. Also stability of the steady-state solutions can be verified. The transfer of energy from one to another mode of vibrations is illustrated.

Keywords Kinematic excitation · Resonance · Asymptotic analysis · Multiple-scale method

1 Introduction

Kinematic excitation appears in many problems of applied mechanics and is crucial in some technical problems. It can be induced by contact forces in some devices, mechanisms, vehicles or in civil engineering constructions. Moreover, supports of machines can be exposed to the kinematic excitation through vibrations of basement caused by road or railway traffic, seismic vibration or another machine neighborhood.

There are many examples of problems with kinematic excitation in literature. The dynamic investigations of low structures subject to kinematic excitation caused by transverse waves are described in [4]. Severe interaction between the bogie of a modern railway passenger car and the track caused by kinematic and parametric excitation from the track and by kinematic excitation due to wheel tread polygonalization are studied in [6]. The dynamic behavior of a self-propelled equipment due to kinematic excitation caused by a bumpy road is examined in [2]. Such problems are also found in nano scale. In [3] the possibility of the existence of undamped kinematic excitation in one-dimensional molecular crystals is tested.

Many authors test the behavior of various kinds of pendulum as a good and intuitive example of a nonlinear system [5, 7–9]. In the paper [1], the chaotic response of a harmonically excited spring pendulum that is moving in circular path is studied. This is a nonlinear multi-degree-of-freedom system and it is a good example for several engineering applications such as ship motion.

In this paper also a kind of a pendulum is tested. This is a spring pendulum with suspension point moving in a prescribed path. Apart from this kinematic excitation and assumed external forces, the inertial coupling can lead to autoparametric excitation of vibrations. The two degree-of-freedom system investigated in the paper is a good example to develop

R. Starosta (✉) · G. Sypniewska-Kamińska
Institute of Applied Mechanics, Poznan University of Technology, ul. Piotrowo 3, 60-965 Poznań, Poland
e-mail: roman.starosta@put.poznan.pl

J. Awrejcewicz
Department of Automation and Biomechanics, Technical University of Łódź, ul. Stefanowskiego 1/15, 90-924 Łódź, Poland

Published online: 19 October 2011

and test the analytical methods due to its simplicity and intuitive predictability. In this paper we focus on detecting resonances conditions and then the chosen case of resonances occurring simultaneously is studied. The applied multiple-scale method allows one to find the number of all possible steady-state amplitudes for the chosen parameters and predict their values. The amplitude-frequency graphs are presented in the case of two resonances occurring simultaneously.

The calculations were made with the use of computer algebra and symbolic manipulation system *Mathematica*. Most operations are made automatically using special procedures created by the authors.

2 Formulation of the problem

We adopt the asymptotic method of multiple scale in order to perform the analytical calculations. A spring pendulum with a moving suspension point is the tested model. The system studied is presented in Fig. 1. The suspension point moves harmonically and independently in two mutually perpendicular directions. Kinematic equations of its motion are

$$x = R_x \cos(\Omega_x t), \qquad y = R_y \sin(\Omega_y t), \tag{1}$$

where R_x, R_y, Ω_x, and Ω_y are known parameters.

As result, the suspension point moves along a Lissajous curve.

We assume that the motion of the whole system is planar. The spring elongation Z and the angle ϕ were chosen as generalized coordinates. Besides kinematic excitation, the moment $M(t) = M_0 \cos(t\Omega_2)$ and the linear viscous damping moment $M_r = C_2\dot{\varphi}$ act around the point O. Moreover, the force $F(t) = F_0 \cos(t\Omega_1)$ and the linear viscous damping $F_r = C_1\dot{X}$ act on the mass m along the pendulum length (C_1 and C_2 are the viscous coefficients). The spring is assumed to be massless and linear with stiffness k.

The equations of motion were derived from Lagrange equations of the second type:

$$\begin{aligned} \frac{d}{dt}\left(\frac{\partial L}{\partial \dot{Z}}\right) - \left(\frac{\partial L}{\partial Z}\right) &= Q_z, \\ \frac{d}{dt}\left(\frac{\partial L}{\partial \dot{\varphi}}\right) - \left(\frac{\partial L}{\partial \varphi}\right) &= Q_\varphi, \end{aligned} \tag{2}$$

where $L = T - V$ denotes the Lagrangian. The potential and kinetic energy of the system reads

$$V = \frac{1}{2}kZ^2 - mg\big(R_x \cos(\Omega_x t) + (L_0 + Z)\cos(\varphi)\big), \tag{3}$$

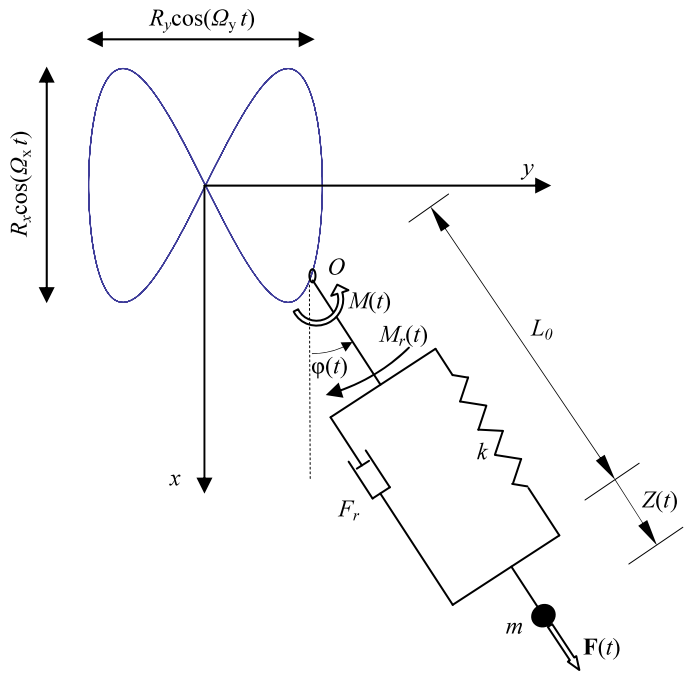

Fig. 1 Spring pendulum moving on a prescribed path

$$
\begin{aligned}
T = {} & \frac{m}{2}\big(R_x^2\Omega_x^2\sin^2(\Omega_x t) + R_y^2\Omega_y^2\cos^2(\Omega_x t)\big) \\
& + m\dot{Z}\big(R_y\Omega_y\sin(\varphi)\cos(\Omega_y t) \\
& - R_x\Omega_x\cos(\varphi)\sin(\Omega_x t)\big) \\
& + m(L_0+Z)\big(R_y\Omega_y\cos(\varphi)\cos(\Omega_y t) \\
& + R_x\Omega_x\sin(\varphi)\sin(\Omega_x t)\big)\dot{\varphi} \\
& + \frac{m}{2}(L_0+Z)^2\dot{\varphi}^2 + \frac{m}{2}\dot{Z}^2. \qquad (4)
\end{aligned}
$$

L_0 is the length of not stretched spring and g denotes Earth's acceleration.

Generalized forces from all nonconservative loads are

$$
\begin{aligned}
Q_z &= F_0\cos(\Omega_1 t) - C_1\dot{Z}, \\
Q_\varphi &= M_0\cos(\Omega_2 t) - C_2\dot{\varphi}. \qquad (5)
\end{aligned}
$$

Introducing (3)–(5) into (2) we get

$$
\begin{aligned}
& -m\big(g + R_x\Omega_x^2\cos(\Omega_x t)\big)\cos\varphi \\
& \quad - mR_y\Omega_y^2\sin(\Omega_y t)\sin\varphi \\
& \quad + C_1\dot{Z} - L_0 m\dot{\varphi}^2 + Z\big(k - m\dot{\varphi}^2\big) + m\ddot{Z} \\
& = F_0\cos(\Omega_1 t), \qquad (6) \\
& m(L_0+Z)\big(-R_y\Omega_y^2\sin(\Omega_y t)\cos\varphi \\
& \quad + \big(g + R_x\Omega_x^2\cos(\Omega_x t)\big)\sin\varphi + 2\dot{Z}\dot{\varphi}\big) \\
& \quad + C_2 L\dot{\varphi} + (L_0+Z)^2 m\ddot{\varphi} = M_0\cos(\Omega_2 t). \qquad (7)
\end{aligned}
$$

Equations (6)–(7) should be supplemented by the initial conditions for generalized coordinates and their first derivatives

$$
\begin{aligned}
Z(0) &= Z_0, \qquad \dot{Z}(0) = V_0, \\
\varphi(0) &= \varphi_0, \qquad \dot{\varphi}(0) = \omega_0, \qquad (8)
\end{aligned}
$$

where $Z_0, V_0, \varphi_0, \omega_0$ are known values.

The problem is then transformed to the dimensionless form. The dimensionless generalized coordinate

$$
z = \frac{Z - \delta_{\mathrm{st}}}{L} \qquad (9)
$$

where $L = L_0 + \delta_{\mathrm{st}}$ is the length of the pendulum at the static equilibrium position, and $\delta_{\mathrm{st}} = \frac{mg}{k}$ is the static elongation. The dimensionless time τ is defined as

$$
\tau = \omega_1 t, \qquad (10)
$$

where $\omega_1^2 = \frac{k}{m}$.

The dimensionless frequencies are assumed as follows:

$$
\begin{aligned}
& w = \frac{\omega_2}{\omega_1}, \qquad p_1 = \frac{\Omega_1}{\omega_1}, \qquad p_2 = \frac{\Omega_2}{\omega_1}, \\
& p_x = \frac{\Omega_x}{\omega_1}, \qquad p_y = \frac{\Omega_y}{\omega_1}, \qquad (11)
\end{aligned}
$$

where $\omega_2^2 = \frac{g}{L}$.

The other parameters are assumed in the form

$$
\begin{aligned}
& r_x = \frac{R_x}{L}, \qquad r_y = \frac{R_y}{L}, \qquad c_1 = \frac{C_1}{m\omega_1}, \\
& c_2 = \frac{C_2}{mL^2\omega_1}, \qquad f_1 = \frac{F_0}{mL\omega_1^2}, \qquad f_2 = \frac{M_0}{mL^2\omega_1^2}. \qquad (12)
\end{aligned}
$$

According to the above introduced definitions, the governing equations of motion in dimensionless form are

$$
\begin{aligned}
& \ddot{z}(\tau) + c_1\dot{z}(\tau) - \big(1+z(\tau)\big)\big(\dot{\varphi}(t)\big)^2 + z(\tau) \\
& \quad + w^2\big(1 - \cos\big(\varphi(\tau)\big)\big) - r_x p_x^2\cos(\tau p_x)\cos\big(\varphi(\tau)\big) \\
& \quad - r_y p_y^2\sin(\tau p_y)\sin\big(\varphi(\tau)\big) \\
& = f_1\cos(p_1\tau), \qquad (13) \\
& \big(1+z(\tau)\big)^2\ddot{\varphi}(\tau) + \big(c_2 + 2\big(1+z(\tau)\big)\dot{z}(\tau)\big)\dot{\varphi}(\tau) \\
& \quad + w^2\sin\big(\varphi(\tau)\big)\big(1+z(\tau)\big) \\
& \quad - r_y p_y^2\big(1+z(\tau)\big)\sin(\tau p_y)\cos\big(\varphi(\tau)\big) \\
& \quad + r_x p_x^2\big(1+z(\tau)\big)\cos(\tau p_x)\sin\big(\varphi(\tau)\big) \\
& = f_2\cos(p_2\tau), \qquad (14)
\end{aligned}
$$

with initial conditions for nondimensional generalized coordinates and their first derivatives

$$
\begin{aligned}
z(0) &= z_0, \qquad \dot{z}(0) = v_0, \\
\varphi(0) &= \varphi_0, \qquad \dot{\varphi}(0) = \omega_0, \qquad (15)
\end{aligned}
$$

where $z_0 = \frac{Z_0 - \delta_{\mathrm{st}}}{L}$, $v_0 = \frac{V_0}{L\omega_1}$.

3 Asymptotic solution

The multiple-scale method is applied to solve the governing equations and to obtain the resonance conditions. Trigonometric functions of φ in (13)–(14) are

approximated by some first terms of Taylor series in the following way:

$$\sin\varphi \cong \varphi - \frac{1}{3!}\varphi^3, \qquad \cos\varphi \cong 1 - \frac{1}{2}\varphi^2. \tag{16}$$

The approximation (16) is valid in a small neighborhood of the static equilibrium position.

The dumping coefficient and the amplitudes of external loading are estimated as relatively small and then they are assumed as

$$c_i = \varepsilon^2 \tilde{c}_i, \qquad f_i = \varepsilon^3 \tilde{f}_i, \quad i = 1, 2, \tag{17}$$

where ε is the so-called small parameter and $0 < \varepsilon \ll 1$. Moreover, we postulate

$$r_x = \varepsilon^2 \tilde{r}_x, \qquad r_y = \varepsilon^2 \tilde{r}_y. \tag{18}$$

The parameters $\tilde{f}_i, \tilde{c}_i, \tilde{r}$ are of the order 1.

The amplitudes of vibrations are assumed to be of the order of a small parameter ε. Let us introduce some new variables ζ and ϕ

$$z(\tau) = \varepsilon\zeta(\tau;\varepsilon), \qquad \varphi(\tau) = \varepsilon\phi(\tau;\varepsilon). \tag{19}$$

The functions ζ and ϕ are sought in the form

$$\begin{aligned} \zeta(\tau;\varepsilon) &= \sum_{k=1}^{k=3} \varepsilon^k \zeta_k(\tau_0,\tau_1,\tau_2) + O\left(\varepsilon^4\right), \\ \phi(\tau;\varepsilon) &= \sum_{k=1}^{k=3} \varepsilon^k \phi_k(\tau_0,\tau_1,\tau_2) + O\left(\varepsilon^4\right), \end{aligned} \tag{20}$$

where $\tau_0 = \tau$, $\tau_1 = \varepsilon\tau$ and $\tau_2 = \varepsilon^2\tau$ are various time scales.

The derivatives with respect to time τ are calculated in terms of the new time scales as follows:

$$\begin{aligned} \frac{d}{d\tau} &= \frac{\partial}{\partial\tau_0} + \varepsilon\frac{\partial}{\partial\tau_1} + \varepsilon^2\frac{\partial}{\partial\tau_2}, \\ \frac{d^2}{d\tau^2} &= \frac{\partial^2}{\partial\tau_0^2} + 2\varepsilon\frac{\partial^2}{\partial\tau_0\partial\tau_1} \\ &\quad + \varepsilon^2\left(\frac{\partial^2}{\partial\tau_1^2} + 2\frac{\partial^2}{\partial\tau_0\partial\tau_2}\right) + o\left(\varepsilon^3\right). \end{aligned} \tag{21}$$

Introducing (16)–(18) and (19)–(20) into (13)–(14) and next replacing the ordinary derivatives by the differential operators (21) we obtain two equations in which the small parameter ε appears. These equations should be satisfied for any value of the small parameter, so after ordering the equations due to the powers of ε we get

– the equations of order ε^1

$$\frac{\partial^2\zeta_1}{\partial\tau_0^2} + \zeta_1 = 0, \tag{22}$$

$$\frac{\partial^2\phi_1}{\partial\tau_0^2} + w^2\phi_1 = 0, \tag{23}$$

– the equations of order ε^2

$$\begin{aligned} \frac{\partial^2\zeta_2}{\partial\tau_0^2} + \zeta_2 &= r_x p_x^2 \cos(p_x\tau_0) - \frac{1}{2}w^2\phi_1^2 \\ &\quad - 2\frac{\partial^2\zeta_1}{\partial\tau_0\partial\tau_1} + \left(\frac{\partial\phi_1}{\partial\tau_0}\right)^2, \end{aligned} \tag{24}$$

$$\begin{aligned} &\frac{\partial^2\phi_2}{\partial\tau_0^2} + w^2\phi_2 \\ &\quad = \tilde{r}_y p_y^2 \sin(p_y\tau_0) - w^2\zeta_1\phi_1 \\ &\qquad - 2\frac{\partial\zeta_1}{\partial\tau_0}\frac{\partial\phi_1}{\partial\tau_0} - 2\zeta_1\frac{\partial^2\phi_1}{\partial\tau_0^2} - 2\frac{\partial^2\phi_1}{\partial\tau_0\partial\tau_1}, \end{aligned} \tag{25}$$

– the equations of order ε^3

$$\begin{aligned} &\frac{\partial^2\zeta_3}{\partial T_0^2} + \zeta_3 \\ &\quad = \tilde{f}_1\cos\tau_0 p_1 + \tilde{r}_y p_y^2\phi_1\sin p_y\tau_0 - w^2\phi_1\phi_2 \\ &\qquad - \frac{\partial\zeta_1^2}{\partial\tau_1^2} - \tilde{c}_1\frac{\partial\zeta_1}{\partial\tau_0} + 2\frac{\partial\phi_1}{\partial\tau_1}\frac{\partial\phi_1}{\partial\tau_0} + \zeta_1\left(\frac{\partial\phi_1}{\partial\tau_0}\right)^2 \\ &\qquad + 2\frac{\partial\phi_1}{\partial\tau_0}\frac{\partial\phi_2}{\partial\tau_0} - 2\frac{\partial^2\zeta_1}{\partial\tau_0\partial\tau_2} - 2\frac{\partial^2\zeta_2}{\partial\tau_0\partial\tau_1}, \end{aligned} \tag{26}$$

$$\begin{aligned} &\frac{\partial^2\phi_3}{\partial\tau_0^2} + w^2\phi_3 \\ &\quad = \tilde{f}_2\cos\tau_0 p_2 + \tilde{r}_y p_y^2\zeta_1\sin\tau_0 p_y \\ &\qquad - \tilde{r}_x p_x^2\phi_1\cos\tau_0 p_x - w^2\zeta_2\phi_1 - +\frac{1}{6}w^2\phi_1^3 \\ &\qquad - w^2\zeta_1\phi_2 - \frac{\partial^2\phi_1}{\partial\tau_1^2} - 2\frac{\partial\zeta_1}{\partial\tau_0}\frac{\partial\phi_1}{\partial\tau_1} - \tilde{c}_2\frac{\partial\phi_1}{\partial\tau_0} \\ &\qquad - 2\frac{\partial\zeta_1}{\partial\tau_1}\frac{\partial\phi_1}{\partial\tau_0} - 2\zeta_1\frac{\partial\zeta_1}{\partial\tau_0}\frac{\partial\phi_1}{\partial\tau_0} - 2\frac{\partial\zeta_2}{\partial\tau_0}\frac{\partial\phi_1}{\partial\tau_0} \end{aligned}$$

$$-2\frac{\partial\zeta_1}{\partial\tau_0}\frac{\partial\phi_2}{\partial\tau_0}-2\frac{\partial^2\phi_1}{\partial\tau_0\partial\tau_2}-4\zeta_1\frac{\partial^2\phi_1}{\partial\tau_0\partial\tau_1}$$
$$-2\frac{\partial^2\phi_2}{\partial\tau_0\partial\tau_1}-\zeta_1{}^2\frac{\partial^2\phi_1}{\partial\tau_0^2}-2\zeta_2\frac{\partial^2\phi_1}{\partial\tau_0^2}$$
$$-2\zeta_1\frac{\partial^2\phi_2}{\partial\tau_0^2}. \tag{27}$$

Thus, in accordance with (20), the original equations of motion have been approximated by the set of partial linear differential equations.

The solutions of (22)–(23) are

$$\zeta_1 = A_1(\tau_1,\tau_2)e^{i\tau_0}+\bar{A}_1(\tau_1,\tau_2)e^{-i\tau_0}, \tag{28}$$
$$\phi_1 = A_2(\tau_1,\tau_2)e^{iw\tau_0}+\bar{A}_2(\tau_1,\tau_2)e^{-iw\tau_0}, \tag{29}$$

where A_1 and A_2 are unknown complex functions of slow time scales.

Introducing the first order solutions (28)–(29) into (24)–(25) and then eliminating the secular terms from them, leads to the equations whose solutions have the following form:

$$\zeta_2 = w^2A_2\bar{A}_2-\frac{e^{i\tau_0p_x}\tilde{r}_xp_x^2}{2(p_x^2-1)}+\frac{3e^{i\tau_0w}A_2^2}{2(4w^2-1)}+CC, \tag{30}$$

$$\phi_2 = \frac{ie^{ip_y\tau_0}\tilde{r}_yp_y^2}{2(p_y^2-w^2)}-\frac{e^{i\tau_0(1+w)}w(2+w)A_1A_2}{1+2w}$$
$$+\frac{e^{i\tau_0(1-w)}w(2-w)A_1\bar{A}_2}{1-2w}+CC, \tag{31}$$

where CC stands for the complex conjugates of the preceding terms.

After introducing (28)–(31) into (26)–(27) and omitting secular terms, the third order approximations read

$$\zeta_3 = -\frac{e^{i(1+2w)\tau_0}w(w-1)A_1A_2^2}{4(1+2w)}$$
$$+\frac{e^{i(1-2w)\tau_0}w(w+1)A_1\bar{A}_2^2}{4(2w-1)}+\frac{e^{ip_1\tau_0}\tilde{f}_1}{2(1-p_1^2)}$$
$$+\frac{i\tilde{r}_yp_y^4e^{i(p_y+w)\tau_0}A_2}{2(p_y^2-w^2)((p_y+w)^2-1)}$$
$$+\frac{i\tilde{r}_yp_y^4e^{i(p_y-w)\tau_0}\bar{A}_2}{2(p_y^2-w^2)((p_y-w)^2-1)}+CC, \tag{32}$$

$$\phi_3 = -\frac{e^{i(2+w)\tau_0}w(2+3w+w^2)A_1^2A_2}{4(2w+1)}$$
$$-\frac{e^{i(2-w)\tau_0}w(2-3w+w^2)A_1^2\bar{A}_2}{4(2w-1)}$$
$$-\frac{e^{3iw\tau_0}(13w^2-1)A_2^3}{48(4w^2-1)}+\frac{e^{ip_2\tau_0}\tilde{f}_2}{2(w^2-p_2^2)}$$
$$+\frac{i\tilde{r}_yp_y^4e^{i(1+p_y)\tau_0}A_1}{2(p_y^2-w^2)((p_2+1)^2-w^2)}$$
$$-\frac{i\tilde{r}_yp_y^4e^{i(1-p_y)\tau_0}A_1}{2(p_y^2-w^2)((p_y-1)^2-w^2)}$$
$$+\frac{\tilde{r}_xp_x(p_x^2+w^2-1)e^{i(p_x-w)\tau_0}A_2}{2(p_x^2-1)(p_x-2w)}$$
$$+\frac{\tilde{r}_xp_x(p_x^2+w^2-1)e^{i(p_x+w)\tau_0}A_2}{2(p_x^2-1)(p_x+2w)}+CC. \tag{33}$$

The functions A_1 and A_2 can be calculated from conditions of elimination of secular terms and from the conditions which are consistent with (15).

4 Modulation problem near resonances

The solutions (30)–(33) break down when any of their denominators comes to zero. It is caused by the new secular terms occurring on the right-hand sides of (24)–(27) when some frequency conditions are fulfilled. All resonances till the third order can be recognized in this way. They can be classified as follows:

- main (primary) external resonances when $p_x \approx 1$, $p_2 \approx w$,
- resonance of the spring caused by kinematic excitation when $p_x = 1$,
- resonance of the pendulum caused by kinematic excitation when $p_y = w$ or $p_x = 2w$,
- internal resonance when $1 = 2w$,
- combined resonances when $p_y = \pm(1-w)$, $p_y = \pm(1+w)$.

If the natural frequencies satisfy the above resonance conditions, the system behavior is very complex. Let us examine parametric and primary resonances appearing simultaneously, i.e.

$$p_x \approx 1, \qquad p_2 \approx w. \tag{34}$$

In order to study the resonances, we introduce the new so-called detuning parameters σ_1 and σ_2 as a measure of the distance from the strict resonance:

$$p_x = 1 + \sigma_1 = 1 + \varepsilon\tilde{\sigma}_1 \quad \text{and} \quad p_2 = w + \sigma_2 = w + \varepsilon\tilde{\sigma}_2. \tag{35}$$

Using the resonance conditions (35) in (24)–(27) leads to appearance of secular terms.

Their removal requires now:

– for the second order equations

$$-\frac{1}{2}e^{i\tau_1\tilde{\sigma}_1}\tilde{r}_x p_x^2 + 2i\frac{\partial A_1}{\partial \tau_1} = 0, \tag{36}$$

$$2iw\frac{\partial A_2}{\partial \tau_1} = 0, \tag{37}$$

– for the third order equations

$$i\tilde{c}_1 A_1 + \frac{2A_1 A_2 \bar{A}_2 w^2(7w-1)}{1-4w^2} + 2i\frac{\partial A_1}{\partial \tau_2} = 0, \tag{38}$$

$$-\frac{1}{2}e^{i\tilde{\sigma}_2\tau_1}\tilde{f}_2 + i\tilde{c}_2 w A_2 - \frac{A_1\bar{A}_1 A_2 w^2(7w^2-2)}{-1+4w^2} - \frac{A_2^2\bar{A}_2 w^4(1+8w^2)}{-2+8w^2} + 2iw\frac{\partial A_2}{\partial \tau_2} = 0. \tag{39}$$

The above formulas are so-called solvability conditions. From the system of (36)–(39) the unknown functions $A_1(\tau_1,\tau_2)$, $\bar{A}_1(\tau_1,\tau_2)$, $A_2(\tau_1,\tau_2)$, $\bar{A}_2(\tau_1,\tau_2)$ can be found.

For further calculations they are presented in the polar representation

$$A_1(\tau_1,\tau_2) \to \frac{\tilde{a}_1(\tau_1,\tau_2)}{2}e^{i\psi_1(\tau_1,\tau_2)}, \quad A_2(\tau_1,\tau_2) \to \frac{\tilde{a}_2(\tau_1,\tau_2)}{2}e^{i\psi_2(\tau_1,\tau_2)}, \tag{40}$$

where $\tilde{a}_1, \tilde{a}_2$ and ψ_1, ψ_2 are real functions and denote the amplitudes and the phases, respectively, of the solutions ζ, ϕ.

After introducing modified phases

$$\theta_1(\tau_1,\tau_2) = \tau_1\tilde{\sigma}_1 - \psi_1(\tau_1,\tau_2), \quad \theta_2(\tau_1,\tau_2) = \tau_1\tilde{\sigma}_2 - \psi_2(\tau_1,\tau_2), \tag{41}$$

and using definition (21), the partial differential equations (36)–(39) are transformed to the ordinary differential equations

$$i\frac{da_1}{d\tau} + a_1\left(-\sigma_1 + \frac{d\theta_1}{d\tau}\right) = -\frac{1}{2}ia_1c_1 + \frac{1-7w^2}{4(1-4w^2)}w^2a_1a_2^2 + \frac{r_x p_x^2}{2}(\cos\theta_1 + i\sin\theta_1), \tag{42}$$

$$i\frac{da_2}{d\tau} + a_2\left(-\sigma_2 + \frac{d\theta_2}{d\tau}\right) = -\frac{1}{2}ia_2c_2 + \frac{7w^2-1}{4(4w^2-1)}wa_2a_1^2 + \frac{8w^4+5w^2-1}{16(4w^2-1)}wa_2^3 + \frac{f_2}{2w}(\cos\theta_2 + i\sin\theta_2). \tag{43}$$

Thanks to the definitions (41), the above modulation system is autonomous. The original denotations of the system parameters are used again in (42)–(43) according to (17), (18), and (35). The quantities $a_i = \varepsilon\tilde{a}_i$ are amplitudes of the original functions z, ϕ. However, both phases ψ_i and the modified phases θ_i are the same for the original functions z, φ and for ζ, ϕ.

Comparison of the real and imaginary parts of both sides of the above equations leads to four equations with respect to amplitudes a_1, a_2 and modified phases θ_1, θ_2:

$$a_1\frac{d\theta_1}{d\tau} = a_1\sigma_1 + \frac{7w^2-1}{4(4w^2-1)}w^2a_1a_2^2 + \frac{r_x(1+\sigma_1)^2}{2}\cos\theta_1, \tag{44}$$

$$\frac{da_1}{d\tau} = -\frac{1}{2}a_1c_1 + \frac{r_x(1+\sigma_1)^2}{2}\sin\theta_1, \tag{45}$$

$$a_2\frac{d\theta_2}{d\tau} = \sigma_2a_2 + \frac{7w^2-1}{4(4w^2-1)}wa_2a_1^2 + \frac{8w^4+5w^2-1}{16(4w^2-1)}wa_2^3 + \frac{f_2}{2w}\cos\theta_2, \tag{46}$$

$$\frac{da_2}{d\tau} = -\frac{1}{2}a_2c_2 + \frac{f_2}{2w}\sin\theta_2. \tag{47}$$

The above set of equations describes modulation of the amplitudes and the modified phases for the tested case of two resonances occurring simultaneously. The

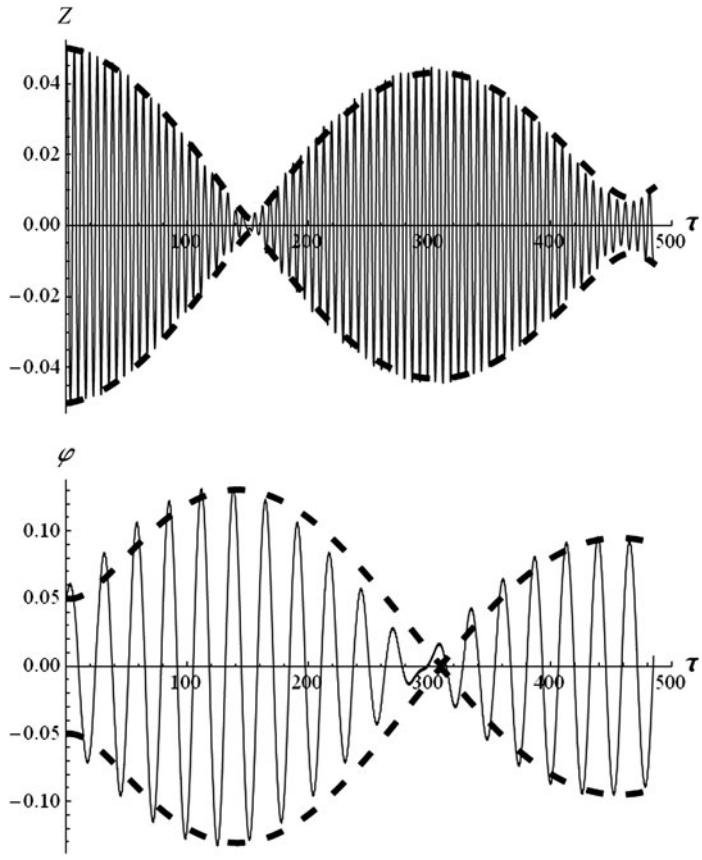

Fig. 2 Time history together with curves of amplitude modulation

solutions of (44)–(47) for chosen values of the system parameters are presented graphically in Fig. 2. The dashed lines show the modulation of the amplitudes for generalized coordinates z and φ. However, the continuous lines represent the time history of vibrations which were obtained numerically as solutions of the original problem (13)–(15). The solutions presented in the graphs were obtained by adopting the following values of parameters: $\sigma_1 = -0.02$, $\sigma_2 = 0.02$, $w = 0.23$, $p_x = 1+\sigma_1$, $p_2 = w+\sigma_2$, $p_1 = 1.76$, $p_y = 7.3$, $f_1 = 0.001$, $f_2 = 0.0005$, $c_1 = 0.002$, $c_2 = 0.004$, $r_x = 0.001$, $r_y = 0.001$.

The mean square error relative to the norm of the function extreme values is applied in order to evaluate the accuracy of the obtained results. The error is calculated as follows:

$$E_j = \sqrt{\frac{\frac{1}{n_j}\sum_{i=1}^{n_j}(a_j(\tau_i) - \widehat{a}_j(\tau_i))^2}{\frac{1}{n_j}\sum_{i=1}^{n_j}(\widehat{a}_j(\tau_i))^2}}, \quad j = 1, 2$$

where $\widehat{a}_j(t_i)$ are extrema of the functions $z(t)$ for $j = 1$ and $\varphi(t)$ for $j = 2$, t_i are the instants at which these extrema occur, $\tau_i \in (0, \tau_{\max})$, $\tau_{\max}$ is time of the simulation, n_j is the total number of the extrema in $(0, \tau_{\max})$.

The errors for longitudinal and swing vibrations were calculated in the interval $(0, 5000)$. Their values are

$$E_1 = 0.0128, \qquad E_2 = 0.0471.$$

The intensive energy exchange between modes of vibrations and energy transfer between the system and the source of external loading including kinematic excitation are observable.

5 Steady-state solution

Steady-state vibrations establish when transient processes disappear due to the damping of the system. The amplitudes and modified phases of steady-state solution correspond to zero values of the derivatives in (44)–(47).

After the elimination of the modified phases θ_1 and θ_2 from steady-state solution, the frequency response functions are derived:

– for parametric resonance

$$a_1^2\left(\frac{w^2(7w^2-1)a_2^2}{4(1-4w^2)}-\sigma_1\right)^2+\frac{c_1^2}{4}a_1^2 - \frac{r_x^2(1+\sigma_1)^4}{4}=0, \tag{48}$$

– for external resonance

$$a_2^2\left(-\sigma_2+\frac{(7w^2-1)wa_1^2}{4(1-4w^2)} + \frac{(1-5w^2+8w^4)wa_2^2}{16(1-4w^2)}\right)^2 + \frac{c_2^2}{4}a_2^2-\frac{f_2^2}{4w^2}=0, \tag{49}$$

where a_1 and a_2 are amplitudes of the longitudinal and swing vibrations, respectively.

When two resonances appear simultaneously then the implicit relations (48) and (49) should be treated as a set of non-linear algebraic equations with respect to variables: a_1, a_2. It can have up to seven pairs of real solutions. All possible steady-state solutions near resonance can be illustrated on the plane of coordinates a_1, a_2. In Fig. 3 the dashed lines are the geometric place of the roots of (48), and the continuous one indicates solutions of (49). The intersection points of both curves represent the solution of the set (48)–(49). Therefore the coordinates a_1 and a_2 of the intersection points of both curves in Fig. 3 show the steady-state amplitudes of longitudinal and swing vibrations, respectively. The steady states of vibration determined in this way may be stable or not.

The graphical solution of the set (48)–(49) which is presented in Fig. 3 was obtained for the following parameters: $w = 0.23$, $f_2 = 0.001$, $c_1 = 0.002$, $c_2 = 0.003$, $r_x = 0.002$.

The number of possible solutions (amplitudes), strongly depends on parameters of the vibrating system. The minimum number of the possible amplitudes is 1 and the maximum number equals 7, which is observable in Fig. 3.

The amplitude-frequency responses are presented in Figs. 4, 5 for the same values of parameters as above. The amplitudes indicated in Fig. 3 are marked also in Figs. 4 and 5.

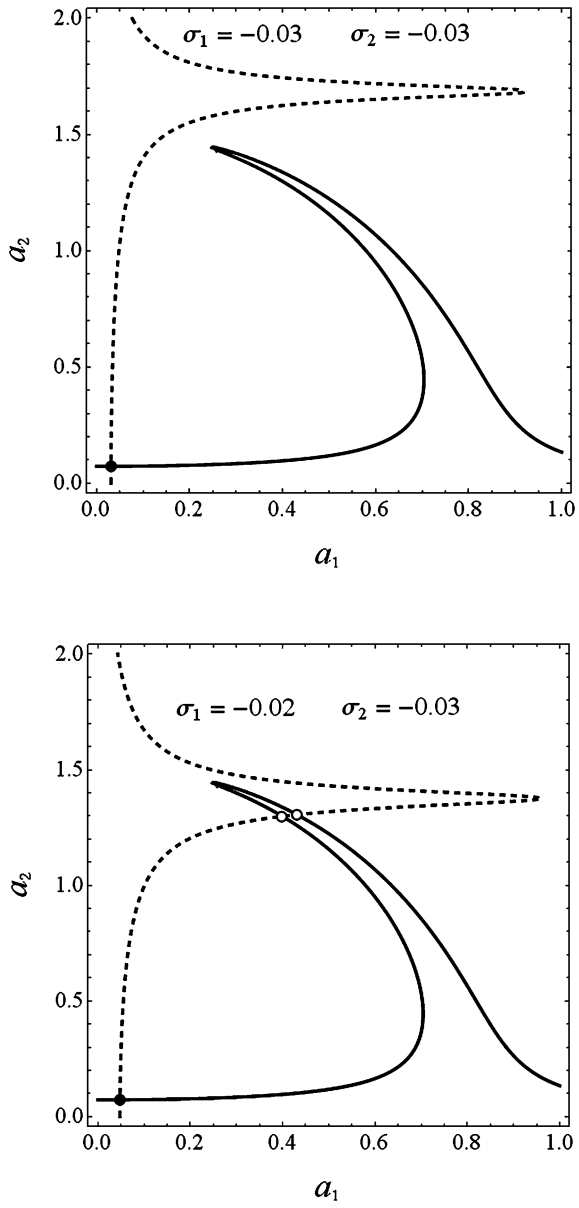

Fig. 3 Graphical presentation of all possible steady-state amplitudes for chosen parameters

The number of possible steady-state amplitudes depends among others on the value of damping. In Fig. 6, it is clearly shown how their number changes with c_2. The other parameters are as follows: $\sigma_1 = -0.01$, $\sigma_2 = -0.04$, $w = 0.23$, $f_2 = 0.004$, $c_1 = 0.004$, $r_x = 0.004$. Reducing damping can increase the number of possible steady-state amplitudes in the area of resonance.

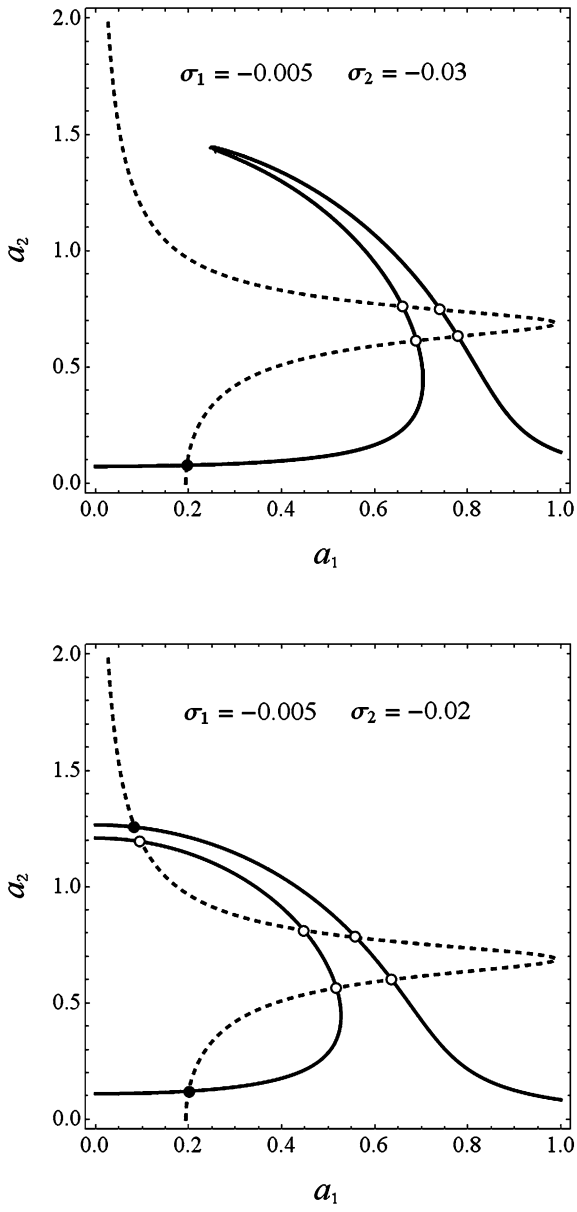

Fig. 3 (*Continued*)

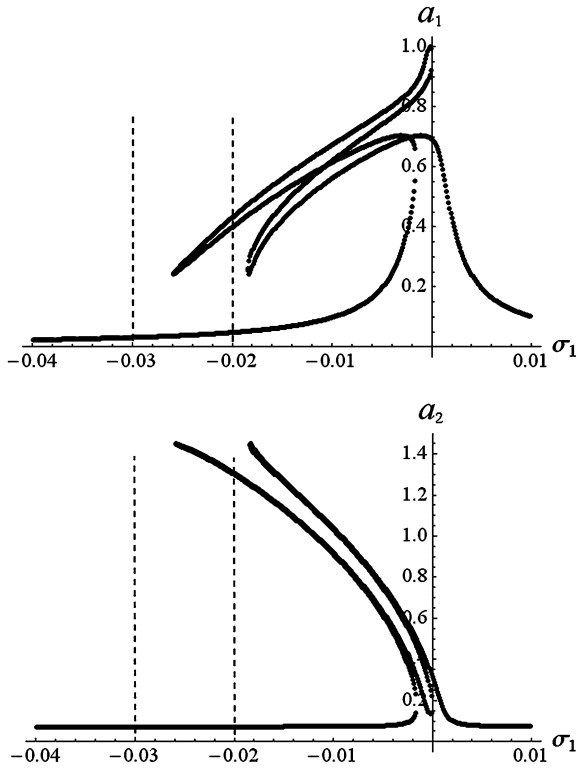

Fig. 4 Amplitude curves versus σ_1 for $\sigma_2 = -0.03$

6 Stability

The separate and important aspect of the problem of the steady-state vibrations is their stability. In order to study this problem we can analyze the behavior of the system in close neighborhood of the fixed points.

To analyze the stability of the particular steady-state solution, the following substitutions are introduced into the set (44)–(47):

$$\begin{aligned} a_1 &= a_{10} + a_{11}, \qquad \theta_1 = \theta_{10} + \theta_{11}, \\ a_2 &= a_{20} + a_{21}, \qquad \theta_2 = \theta_{20} + \theta_{21}, \end{aligned} \tag{50}$$

where $a_{10}, \theta_{10}, a_{20}, \theta_{20}$ are steady-state solutions of (44)–(47), and $a_{11}, \theta_{11}, a_{21}, \theta_{21}$ are perturbations which are assumed to be small compared to a_{10}, θ_{10}, a_{20}, θ_{20}. After linearization and using the fact that steady-state solutions are a fixed point of (44)–(47), we get

$$\begin{aligned} a_{10}\frac{d\theta_{11}}{d\tau} = &-\frac{r_x(1+\sigma_1)^2}{2}\sin\theta_{10}\theta_{11} \\ &+\left(\sigma_1 + \frac{7w^2-1}{4(4w^2-1)}w^2a_{20}^2\right)a_{11} \\ &+\frac{7w^2-1}{2(4w^2-1)}w^2a_{10}a_{20}a_{21}, \end{aligned} \tag{51}$$

$$\frac{da_{11}}{d\tau} = \frac{r_x(1+\sigma_1)^2}{2}\cos\theta_{10}\theta_{11} - \frac{1}{2}c_1a_{11}, \tag{52}$$

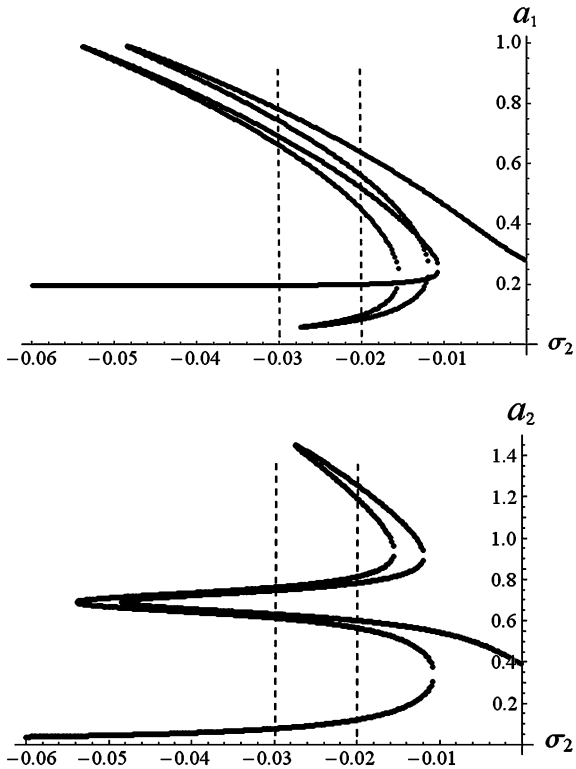

Fig. 5 Amplitude curves versus σ_2 for $\sigma_1 = -0.005$

$$a_{20}\frac{d\theta_{21}}{d\tau} = \frac{7w^2-1}{2(4w^2-1)}wa_{20}a_{10}a_{11} + \left(\frac{7w^2-1}{4(4w^2-1)}wa_{10}^2 + \sigma_2 + \frac{8w^4+5w^2-1}{16(4w^2-1)}3wa_{20}^2\right) - \frac{f_2}{2w}\sin\theta_{20}\theta_{21}, \tag{53}$$

$$\frac{da_{21}}{d\tau} = -\frac{1}{2}c_2a_{21} + \frac{f_2}{2w}\cos\theta_{20}\theta_{21}. \tag{54}$$

The perturbations $a_{11}, \theta_{11}, a_{21}, \theta_{21}$ are unknown functions in the above linear system. Each solution is a linear superposition of the exponential functions $C_i e^{\lambda\tau}$ where C_i are constants and $i = 1, \ldots, 4$.

If the steady-state solution $a_{10}, \theta_{10}, a_{20}, \theta_{20}$ is asymptotically stable, then the real parts of the roots of the characteristic equation of the set (51)–(54),

$$\lambda^4 + \Gamma_1\lambda^3 + \Gamma_2\lambda^2 + \Gamma_3\lambda + \Gamma_4 = 0, \tag{55}$$

should be negative. The coefficients $\Gamma_1, \Gamma_2, \Gamma_3, \Gamma_4$ depend on the parameters $a_{10}, \theta_{10}, a_{20}, \theta_{20}, w, c_1, c_2, r_x, f_2$, and have the form

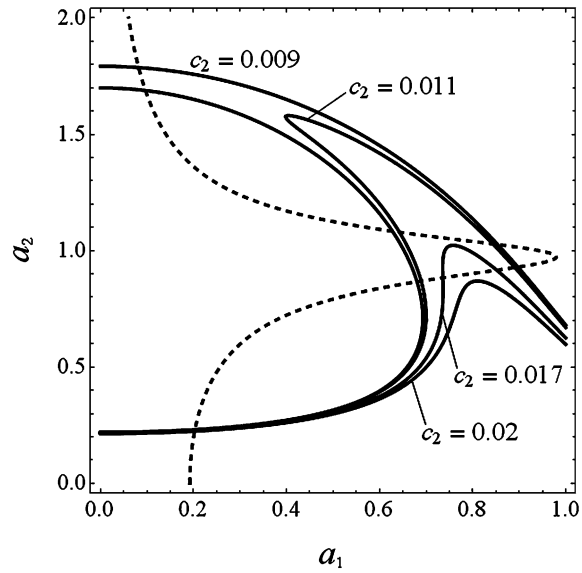

Fig. 6 Graphical solution of the set (45)–(46) for various values of c_2

$$\Gamma_1 = \frac{c_1}{2} + \frac{c_2}{2} + D_2\sin\theta_{10} + D_5\sin\theta_{20},$$

$$\Gamma_2 = \frac{c_1c_2}{4} - a_{20}^2D_1D_2w\cos\theta_{10} - D_2\sigma_1\cos\theta_{10} - D_5\left(a_{10}^2D_1 + 3a_{20}^2D_4 + \sigma_2\right)\cos\theta_{20} + \frac{1}{2}c_1D_2\sin\theta_{10} + \frac{1}{2}c_2D_2\sin\theta_{10} + \frac{1}{2}c_1D_5\sin\theta_{20} + \frac{1}{2}c_2D_5\sin\theta_{20} + D_2D_5\sin\theta_{10}\sin\theta_{20},$$

$$\Gamma_3 = -\frac{1}{2}a_{20}^2c_2D_1D_2w\cos\theta_{10} - \frac{1}{2}c_2D_2\sigma_1\cos\theta_{10} - \frac{1}{2}c_1D_5\left(a_{10}^2D_1 + 3a_{20}^2D_4 + \sigma_2\right)\cos\theta_{20} + \frac{1}{4}c_1c_2D_2\sin\theta_{10} + \frac{1}{4}c_1c_2D_5\sin\theta_{20} + \frac{1}{2}D_2D_5(c_1+c_2)\sin\theta_{10}\sin\theta_{20} + D_2D_5\left(a_{20}^2D_1w + \sigma_1\right)\cos\theta_{10}\sin\theta_{20},$$

$$\Gamma_4 = -4a_{10}^2a_{20}^2D_1^2D_2D_5w\cos\theta_{10}\cos\theta_{20} + D_2D_5\left(a_{10}^2D_1 + 3a_{20}^2D_4 + \sigma_2\right) \times \left(a_{20}^2D_1w + \sigma_1\right)\cos\theta_{10}\cos\theta_{20}$$

$$
\begin{aligned}
&- \frac{1}{2}c_1 D_2 D_5\left(a_{10}^2 D_1 + 3a_{20}^2 D_4 + \sigma_2\right)\\
&\times \cos\theta_{20}\sin\theta_{10}\\
&- \frac{1}{2}c_2 D_2 D_5\left(a_{20}^2 D_1 w + \sigma_1\right)\cos\theta_{10}\sin\theta_{20}\\
&- \frac{1}{4}c_1 c_2 D_2 D_5 \sin\theta_{10}\sin\theta_{20},
\end{aligned}
$$

where

$$
D_1 = \frac{7w^2-1}{4(4w^2-1)}w, \qquad D_2 = \frac{r_x(1+\sigma_1)^2}{2},
$$

$$
D_4 = \frac{8w^4+5w^2-1}{16(4w^2-1)}w, \qquad D_5 = \frac{f_2}{2w}.
$$

According to the Routh–Hurwitz criterion the necessary and sufficient conditions of stability of the particular steady-state solution are

$$
\begin{aligned}
&\Gamma_1 > 0, \qquad \Gamma_3(\Gamma_1\Gamma_2 - \Gamma_3) - \Gamma_4\Gamma_1^2 > 0,\\
&\Gamma_1\Gamma_2 - \Gamma_3 > 0, \qquad \Gamma_4 > 0.
\end{aligned}
\tag{56}
$$

The procedure was used to test stability of the solutions presented in Figs. 3 and 4. The points marked by black dots in Fig. 3 are recognized in this way as stable solutions, and those marked by circles are not stable ones.

7 Conclusions

The non-linear two degree-of-freedom system has been examined. The problem has been transformed to the dimensionless form and the analytical approximate solution has been obtained using multiple-scale method in time domain. The solution till the third order has been achieved. It allows one to detect all possible resonances which can occur in the system. The detailed analysis of the case when parametric and primary resonances appeared simultaneously has been carried out, i.e. when $p_x \approx 1$, $p_2 \approx w$.

For this case the modulation equations have been derived. Their solution is compatible with numerical one. The possible amplitudes of steady-state vibrations have been analytically derived and presented in Figs. 3 and 4. Up to 7 real solutions (amplitudes) have been observed in near neighborhood of simultaneously appearing resonances. The frequency response functions have been obtained from the modulation equations. They are presented in Fig. 5. For possible steady-state solutions of the system the stability analysis was made introducing small perturbations into the modulation equations and taking advantage of Routh–Hurvitz criterion.

The transformations within the multiple-scale-method were carried out automatically with the use of the procedures elaborated and implemented by the authors in software for technical and scientific computing *Mathematica*®.

Acknowledgements J. Awrejcewicz research part has been supported by the Alexander von Humboldt Foundation (Humboldt Award).

References

1. Amer, T., Bek, M.: Chaotic responses of a harmonically excited spring pendulum moving in circular path. Nonlinear Anal. (5), 3196–3202 (2009)
2. Axinti, A., Axinti, G.: About kinematic excitation induced of the dislevelments bed bearer to the wheel of self-propelled equipments. Rom. J. Acoust. Vib. **2**(3), 79–82 (2006)
3. Kozmidis-Luburić, U., Marinković, M., Ćirić, D., Tosić, B.: Undamped kinematical excitations in molecular chains. Physica A **2**(163), 483–490 (1990)
4. Pielorz, A.: Vibrations of discrete-continuous models of low structures with a nonlinear soft spring. J. Theor. Appl. Mech. (39), 153–174 (2001)
5. Starosta, R., Awrejcewicz, J.: Asymptotic analysis of parametrically excited spring pendulum. In: Visa, I. (ed.) Proc. of the 10th IFToMM Symposium—SYROM 2009, Brasov, Romania. Springer, Berlin (2009)
6. Szolc, T.: Simulation of dynamic interaction between the railway bogie and the track in the medium frequency range. Multibody Syst. Dyn. (6), 99–122 (2001)
7. Tondl, A., Nabergoj, R.: Dynamic absorbers for an externally excited pendulum. J. Sound Vib. **234**(4), 611–624 (2000)
8. Weibel, S., Kaper, T., Baillieul, J.: Global dynamics of a rapidly forced cart and pendulum. Nonlinear Dyn. **13**, 131–170 (1997)
9. Zhu, S.J., Zheng, Y.F., Fu, Y.M.: Analysis of non-linear dynamics of a two-degree-of-freedom vibration system with nonlinear damping and non-linear spring. J. Sound Vib. **271**, 15–24 (2004)